A TEMPERATURE-CORRECTED DUAL- LUMINOPHORE PRESSURE-SENSITIVE PAINT SYSTEM

A Thesis

Presented in Partial Fulfillment of the Requirements for

Graduation with Distinction in Aeronautical and Astronautical Engineering

College of Engineering at The Ohio State University

By

Samuel Robert Long

*****

The Ohio State University

2011

Examination Committee:

Dr. James W. Gregory, Advisor

Dr. Jeffery Bons

BLANK PAGE

ABSTRACT

A new pressure-sensitive paint (PSP) system has been developed that can successfully resolve both pressure and temperature contours on a model and it was demonstrated on a NACA 0021 airfoil in a Mach 0.6 flow. Historically PSP measurement systems were susceptible to thermal changes which introduce false pressure data in the results. The oxygen sensor in PSP is also sensitive to temperature changes. The temperature error of the PSP used was quantified as 3 kPa per °C change from the reference condition. To remove or alleviate this source of error, a thermographic phosphor $(Y_{0.99}Ce_{0.01})_2(Ga_{0.75}Al_{0.25})_5O_{12}$ was introduced into the paint mixture. When excited by a pulsed LED array at 480 nm, the phosphor emitted light at a spectrally distinct wavelength centered at 560 nm while PtTTFP emitted light centered at 665 nm. Using a color camera and optical filtering, the thermal information is carried by the green channel and the pressure signal is carried by the red channel. The red channel was normalized by the green and the resulting temperature error was reduced. Alternatively a thermographic map was determined and used to correct the corresponding pressure map utilizing *a priori* and *in situ* calibrations.

ACKNOWLEDGEMENTS

Special thanks to Dr. Gregory of The Ohio State University for his advice and support over the duration of the project.

Special thanks to Dr. Steve Allison of Oak Ridge National Laboratory for his help in analyzing possible phosphors for use with PSP

Special thanks to Rachel Hansel and Dr. Greg Walker of Vanderbilt University for their gracious help with procuring the phosphors used and donating them to the research presented here.

Special thanks to Mark Andio and Daniel Chmielewski of the Ohio State Department of Materials Science and Engineering for their assistance in processing the phosphors for mixing in the paint.

Special thanks to Dr. Juliano, Chris Jensen, and Di Peng for their assistance in conducting the experiments and processing the data along with aiding in data analysis.

VITA

January 23, 1990 . . . . . Born - Columbus, Ohio

2011 . . . . . B.S. Aeronautical and Astronautical Engineering, The Ohio State University

PUBLICATIONS

Research Publications

1. S. Fang, S.R. Long, K.J. Disotell, J.W. Gregory, F.C. Semmelmayer, R.W. Guyton, "Comparison of Unsteady Pressure-Sensitive Paint Measurement Techniques." 27th AIAA Aerodynamic Measurement Technology and Ground Testing Conference. 2010-4919, 2010

2. S. Fang, K.J. Disotell, S.R. Long, J.W. Gregory, F.C. Semmelmayer, R.W. Guyton, "Application of fast-responding pressure-sensitive paint to a hemispherical dome in unsteady transonic flow." J. Experiments in Fluids. 2011

TABLE OF CONTENTS

LIST OF ILLUSTRATIONS

LIST OF NOMENCLATURE

A, B = Stern-Volmer Coefficients

C_p = Pressure Coefficient

D_m = Diffusion Constant

E = Error

G = Gated Intensity

h = Binder Thickness

I = Intensity

I_{ref} = Reference Intensity

$\overline{K}$ = Average Sensitivity Value

M = Mach Number

P = Pressure

P_{ref} = Reference Pressure

T = Temperature

T_{ref} = Reference Temperature

τ_{diff} = Difference in Response Time

INTRODUCTION

Pressure-sensitive paint (PSP) represents a new and very accurate measurement technique for determining the pressure distribution across the painted surface.[1] The pressure distribution is very important for research purposes as it quantifies all of the aerodynamic forces present on a surface. With a known pressure distribution, researchers are able to discern the airflow characteristics and as a result design better aircraft, wind turbines, and other aerodynamically influenced products. PSP is also an important tool for validating computational fluid dynamics, directly comparing pressure fields for both. The primary tradeoff when switching from traditional pressure taps to PSP is that the level of precision in the pressure measurement is reduced by several orders of magnitude. However, PSP is often significantly cheaper than traditional testing through an added factor in simplicity during testing. Despite the initial cost in acquiring the data acquisition and operating equipment, the reduction in the cost of manufacturing the model along with the large drop in the number of pressure transducers required dramatically reduces the test cost. It is important to note that since PSP is an optical based measurement tool, ample optical access to the testing surface is needed for both the camera and the lighting to ensure desirable results.

MOTIVATION

Tests with significant thermal effects

The single largest drawback to PSP use is its sensitivity to thermal changes. Efforts have been made to use PSP in non-standard conditions where thermal gradients are present. In a test by Fang, a large model was tested at a Mach number of 0.6. Even though thermal equilibrium had been establish in the test, a thermal gradient still persisted limiting the precision of the PSP measurements in this thermally sensitive region. Even with the utilization of multiple taps, the thermal effects couldn't be accounted for.[2]

Unsteady pressure variations are often a key area of interest in wind tunnel experimentation as they can greatly affect the performance and stability of an aircraft in addition to being the source of vibrations. Understanding the source of aerodynamic vibrations can enable engineers to avoid resonant frequencies in design along with reducing the acoustic signature of a body in motion. Additionally, the optical sensing method can isolate actual pressure fluctuations discrete from the vibrations of the tunnel itself. Unfortunately unsteady pressure sensitive paints have a higher thermal sensitivity.

Areas of interest outside of traditional PSP

There are numerous areas of research and active wind tunnel testing that occur outside the bounds of current PSP capabilities. PSP has been unable to be used in these new testing environments for a variety of reasons, but a large reason for most of them is the unsteady nature of the testing. A large number of wind tunnels operate in a blow down configuration where high pressure air from a storage tank supplies enough energy to operate the wind tunnel for a short duration at very high speeds. These facilities are

fundamentally cheaper by decreasing the amount of power required to run by sacrificing actual testing time. The Ohio State University Aeronautical and Astronautical Research Lab has two such facilities, one of which has been tested with PSP in the test section.[3] These tunnels operate over a very short duration with dramatic thermal shifts during operation. This tunnel provides an excellent opportunity to test the limits of any particular PSP system.

BACKGROUND

How PSP Works

A typical PSP system contains a luminescent molecule that is sensitive to the partial pressure of oxygen in the air. When a luminophore molecule is excited by a photon of the correct wavelength, the molecule can return to a stable energy level with one of three ways. The first avenue is phonon radiation, vibrational energy transfer among molecules which is throttled by the local temperature within the sensing layer of the paint. The second is oxygen quenching, where an excited luminophore comes into contact with a free radical oxygen molecule which absorbs the excess energy of the luminophore molecule returning it to the ground state. The third is the radiation of a photon. This photon is spectrally distinct from the excitation photon; it is of a longer wavelength due to quantum inefficiency and is known as a Stokes shift in emission. With a constant excitation source, the luminescence of the paint is mitigated by the two variables local temperature and local oxygen concentration. The oxygen concentration is proportional to the partial pressure of oxygen over the paint. If the temperature remains relatively constant from image to image, the error from a thermal change is minimal.

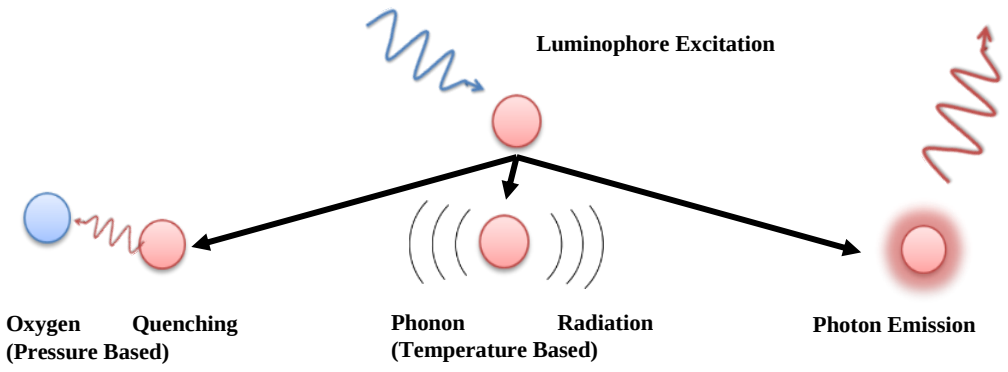

Figure 1. Luminophore Mechanics

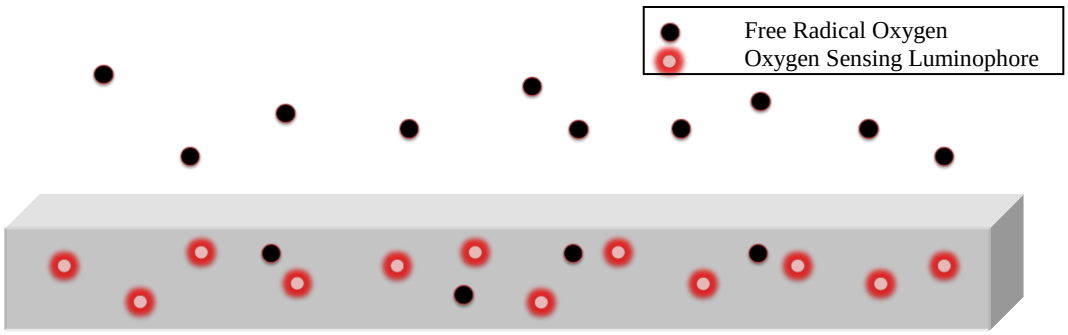

Figure 2. Traditional PSP Setup

Once a paint is prepared, there are several methods that can be used to extract quantitative data from a test. The primary method for acquiring data is an intensity ratio based method. Taking an image while a wind tunnel is on produces an image where each pixel's intensity value reflects the local pressure at that point. However this intensity value is somewhat arbitrary as its value is determined by many factors such as camera exposure time, distance from the camera, local paint thickness, luminophore concentration, the illumination field from the light source along with the pressure and temperature of the paint. To remove most of these errors the image is normalized by a wind off image. Here the pressure is constant across the surface providing a reference point. Additionally any paint imperfections and illumination errors are removed as well by virtue of the referencing method. Using calibrated data from the paint, these intensity ratios can be directly converted to pressures. To increase signal levels, it is common practice to subtract a dark image from every image. This removes the majority of the electronic noise present in the camera. This process is outlined in Figure 3.

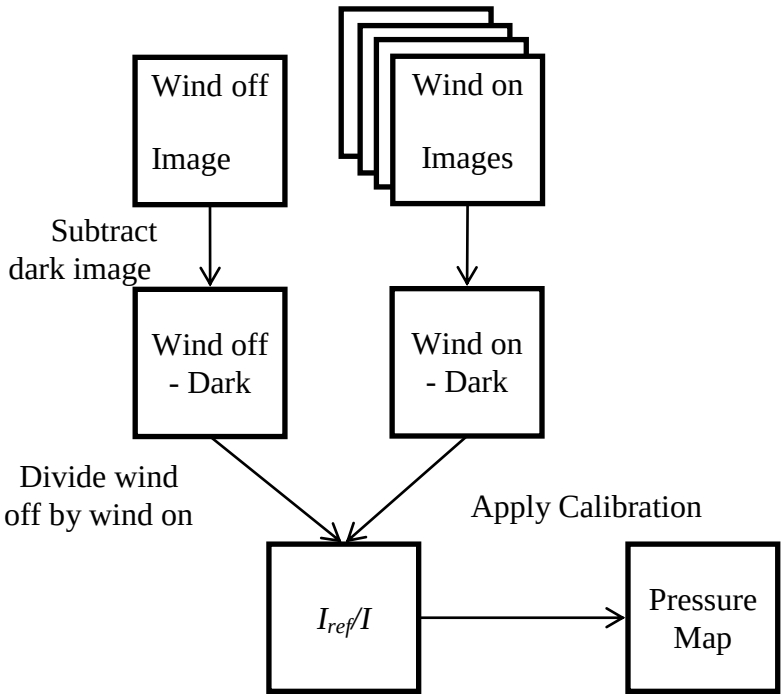

Figure 3. Intensity based method processing

As indicated, these I_{ref}/I values are used directly with calibration results to yield a pressure value. This calibration is known as a Stern-Volmer calibration.

$$\frac{I_{ref}}{I} = B \times \frac{P}{P_{ref}} + A \qquad \textbf{Equation 1}$$

A and *B* are the Stern-Volmer coefficients determined through a linear interpolation of data of corresponding intensity and pressure values. When applying the calibration, the intensity ratio becomes a ratio of the local pressure to the reference pressure. Knowing the reference pressure, the exact pressure can be extracted.

A more advanced version of this technique is designed specifically for the analysis of unsteady pressure fields. This technique locks onto a triggering signal, a high frequency pressure transducer or the measured vibration of the model acts as the signal, and pulses the excitation source at that frequency while the camera shutter is open for a long

duration. The excitation source is then delayed incrementally for each exposure to characterize the entire period of the triggering signal. The series of wind on images are then normalized by wind off images using the same technique as before. The result is a series of images characterizing the unsteady nature of the pressure field at the selected frequency. This method produces a strong signal-to-noise ratio as many pulses of light are averaged together during a single image. This method only shows pressure fluctuations at the frequency selected and all other fluctuations are averaged out.

The second method capable of evaluating unsteady pressure measurements is known as the lifetime method. In this method, two images are taken very close together, one during the excitation pulse, and the second during the decay of the luminescence.

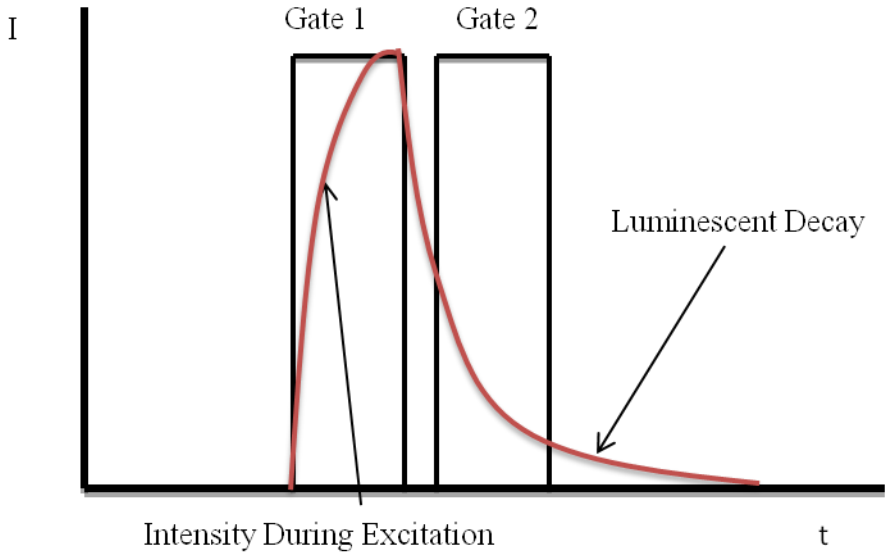

Figure 4. Lifetime Method

The emission of the paint is pressure-insensitive during the excitation pulse while the second image of the decay is dependent on both pressure and temperature, similarly to the intensity-based method. The first image acts as a reference, similar to the wind off image in the intensity-based method enabling a single image pair to be used without a

wind off image. If a wind off image is taken with this method a ratio of ratios can be constructed that is insensitive to most of the testing variables, leaving just pressure and temperature.

$$\frac{I_{ref}}{I} = \frac{\left(G_2 / G_1\right)_{ref}}{\left(G_2 / G_1\right)_{on}} \qquad \textbf{Equation 2}$$

Here the ratio of the gates in the wind on and wind off cases is taken yielding a final intensity ratio expression. This intensity ratio is then used to calibrate the paint in the same Stern-Volmer equation 1. Some of the drawbacks to this method include a lower signal to noise ratio than that of an intensity based method because if one image is taken, and a properly gated in the camera is necessary to observe the pressure sensitivity of the paint. Multiple images may be taken and averaged to improve the signal to noise ratio, but some features may be lost in the averaging process. If a laser is used, the signal to noise issue is partially resolved.

AARL's Custom PSP

The first pressure sensitive paints and the most common commercially available paints are polymer based paints. These paints have 2 parts: an oxygen-permeable polymer binder and an oxygen sensor suspended in the binder. These paints are naturally very stable as the luminophore is located inside of the polymer. However, the response time of the paint is a function of oxygen permeability of the binder, and the thickness of the binder itself. The paint response time is related to these properties by the following equation.

$$\tau_{diff} \propto \frac{h^2}{D_m} \qquad \textbf{Equation 3}$$

τ_{diff} is the response time, h is the binder thickness and D_m is the coefficient of diffusion in the binder. This relation dictates that the time response of a PSP can be controlled by changing the diffusivity of the binder or reducing the thickness. There are several methods to reduce this response time. Most center on reducing the thickness of the binder.

A more recent formulation of PSP, the one which will be used in this research, incorporates a polymer-ceramic mixture as the binder with the luminophore applied to this surface. These paints are a collection of ceramic particles bound together by a minimal amount polymer to create a very porous and strong surface. The advantage of this setup is that the polymer-ceramic binder is very porous and there is an extremely high coefficient of diffusion in the binder as the luminophore is directly applied to the surface as seen in Figure 5. The pressure response, the time it takes for the paint's emission to reflect the pressures present, is purely a function of the luminophore's luminescent decay time. This PSP setup enables testing of unsteady flows and their resulting pressure changes to be measured. The polymer-ceramic allows these unsteady flows to be determined on small time scales on the order of ~10 microseconds. This PSP is explained in greater detail by Gregory *et al*[4].

One drawback of this technique is that the exposed luminophore becomes more sensitive to temperature fluctuation. This is a byproduct of the exposed luminophore molecules in a ceramic structure which means that there is a more efficient heat transfer mechanism than in a purely polymer structure. Because of this more efficient heat

transfer, more luminophore molecules in the excited state would be able to return to their ground state via phonon radiation instead of photon emission. As a result the intensity level of the paint experiences a greater change for an arbitrary temperature shift when compared to a typical polymer substrate. This research aims to reduce or eliminate the temperature induced errors in standard PSP setups.

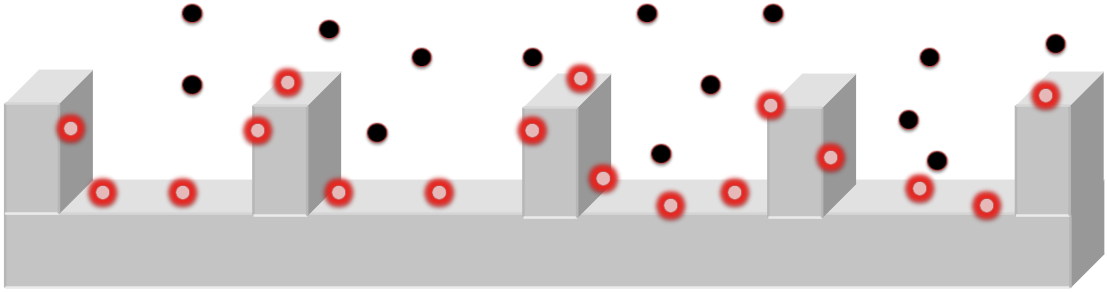

Figure 5. Polymer Ceramic Porous PSP Setup

The Proposed Solution

The temperature sensitivity of the luminophore in PSP is the single largest source of error that affects almost any test involving PSP. This sensitivity can lead to dramatically different indicated pressure measurements as both the intensity and change in intensity per change in pressure drops with increasing temperature. If a temperature shift occurs a two tap correction is used and can mitigate most errors, however temperature gradients often accompany thermal drifts and it is almost impossible to correct the images even when utilizing multiple pressure taps. The new paint studied incorporates a thermographic phosphor into the polymer ceramic substrate to compensate for these temperature effects. This phosphor is spectrally independent of the luminophore, emitting at a peak wavelength of 540 nm versus the luminophore wavelength of 625nm. The paint was sprayed on top of a polymer ceramic base coat followed by the luminophore which results in a surface layout consistent with Figure 6.

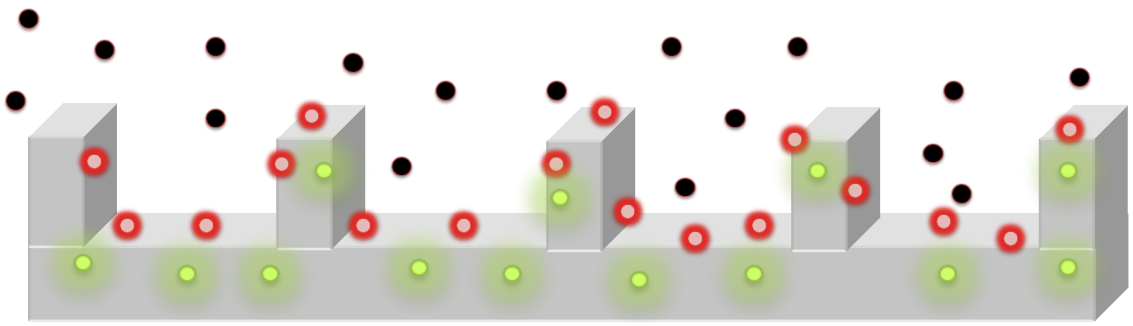

Figure 6. Dual-Luminophore Polymer Ceramic PSP

This setup works on a similar principle as bi-luminophore paints that have been developed for the same purpose detailed by Crafton *et al.*[5] The thermally sensitive, pressure insensitive reference signal is used to remove the temperature dependence of the pressure signal. These paints described by Crafton are fundamentally different as they use organic dyes in the same family of oxygen sensing luminophores versus the ceramic phosphors investigated here. Phosphors offer several advantages over organic dyes. Phosphors have a useful lifetime several orders of magnitude longer than luminescent dyes for two reasons. The first is that luminescent dyes tend to have large complex structures that are more readily broken down when repeatedly excited to energies above its ground state. The second is that dyes can also react with the air, either sublimating away or changing their structure preventing further emissions. The tradeoffs when using phosphors are that they are chemically inert meaning they don't dissolve easily to aid in application. Additionally they don't have the quantum efficiency of dyes leading to lower luminescent levels for similar concentrations.

Thermographic phosphors have been used to determine surface temperature profiles and for remote thermometry.[6] Thermographic phosphors work similarly to oxygen

sensing luminophores used with PSP, either a lifetime or intensity method can be used to remotely determine the surface temperature of the phosphors. There exist a plethora of phosphors in use, each with their own excitation and emission spectra along with a range of temperatures over which they are sensitive. The thermographic phosphor used with the current PSP system had to follow three distinct criteria. It must emit on a spectrally distinct wavelength to separate the temperature signal from the pressure signal. It must utilize the same excitation source to minimize additional sources of error and reduce test setup requirements. Finally it must be thermally sensitive over the testing range of the PSP. Allison examined several thermographic phosphors candidates that followed these criteria.[7]

Of these phosphors, YAG(Ce) appeared to be optimal because it was excited by the same excitation source of 480 nm and emitted on a spectrally distinct peak from common luminophores at 560nm. The only drawback was the phosphor was only thermally sensitive over a range of 50º-200º C, above the normal range PSP testing. However, Hansel[8] substituted gallium for aluminum in the phosphor structure, successfully lowering the quenching temperature to below room temperature levels. These experiments were conducted using a lifetime based method where the quenching temperature is the temperature at which the decay time starts to change significantly as a function of increasing temperature. It is for this reason that initially four phosphors were evaluated.

There are several methods of using a reference signal to compensate for thermal effects. Some of these methods are similar to typical PSP measurements. This first group uses a strictly intensity based method which has been already highlighted earlier. A ratio

of ratios can be created where the wind off - wind on ratio of the reference signal would characterize any thermal drifts and gradients in the test. The wind off – wind on pressure is then normalized by the reference ratio, effectively reducing the thermal sensitivity by the thermal sensitivity of the reference signal. An alternative method would be to use the ratio of the reference signal and through calibration directly determine the temperature on the surface. Then using a 2-d calibration of the pressure signal, find the pressure at that intensity ratio and temperature indicated.

If the lifetime method is used in the measurement process, then a method is proposed by Goss.[9] He suggest that when using a gated signal, if the reference signal lifetime is significantly shorter than that of the pressure signal, only the emission during the excitation pulse will be detected. This emission is directly related to temperature of the paint itself. Once the ratio of the gates is taken, a ratio of ratios is made by normalizing by the reference signal.

PHOSPHOR SELECTION

Experimental Setup

The phosphors under evaluation were first examined visually to estimate their ability to be incorporated into the paint. The particle size had to be small enough such that they could be incorporated into the existing polymer-ceramic paint without affecting the desirable characteristics of the paint. The phosphors were prepared by first grinding them in a mortar and pestle, and suspending them in methanol. Samples of the phosphor were deposited onto thin-layer chromatography (TLC) plates and then placed into the OSU AARL's custom PSP calibration chamber. These phosphors were characterized using an Ocean Optics USB 4000 spectrometer. This chamber offered independent thermal control along with optical access.

Results

The phosphors that were acquired were very similar in nature with subtle difference between each particular phosphor. All of the phosphors were YAG:Ce derivatives with varying doping concentrations of both Cerium and Gallium. The YAG:Ce family of phosphors are all excited by 480nm light and emit at a peak of approximately 550 nm. The only variation between the 4 phosphors was the distinct emission spectra and thermal sensitivity. The phosphors were exercised over the range of the chamber (0-50º C) and the resulting spectra can be seen in Figure 8.

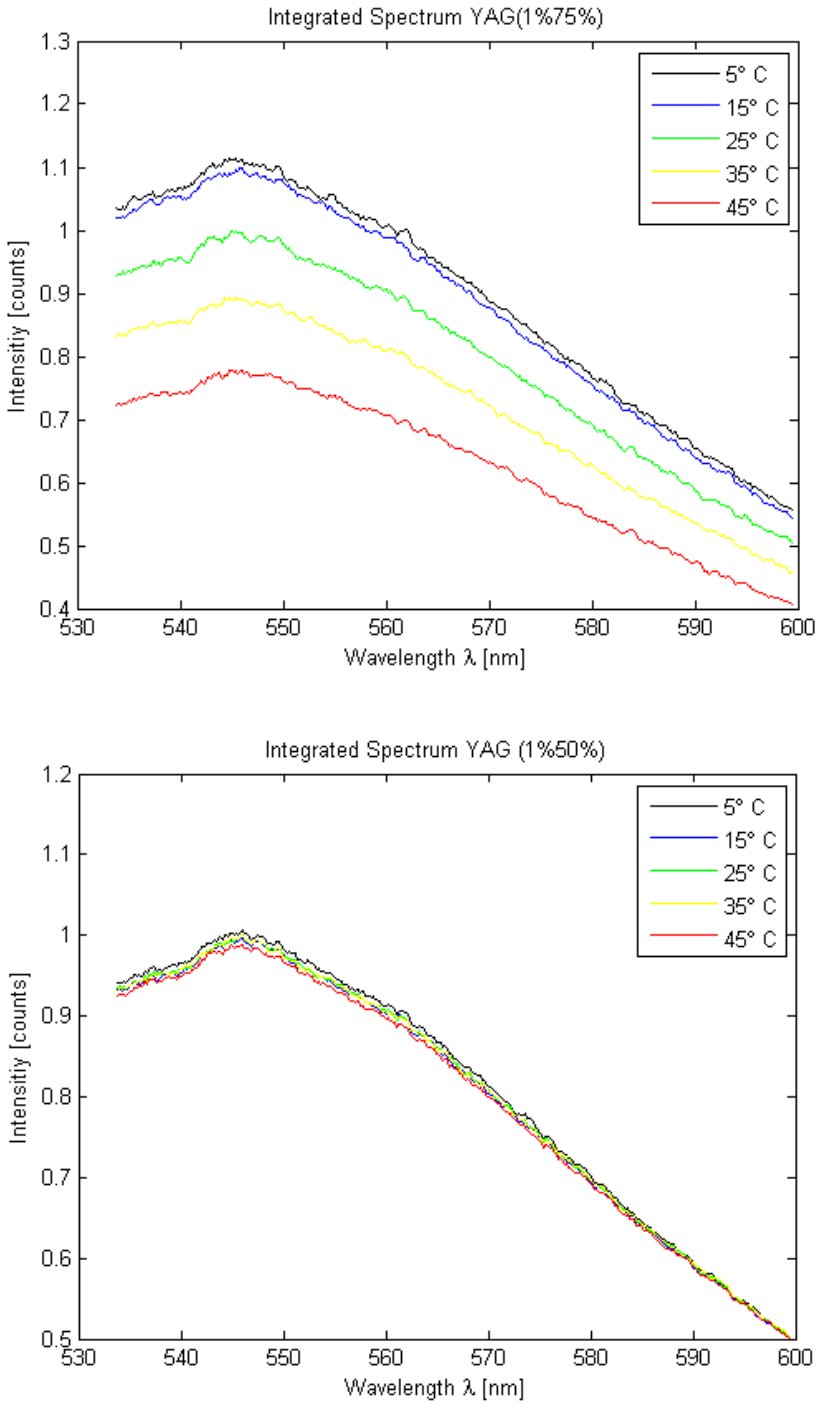

Figure 7. Phosphor Spectra

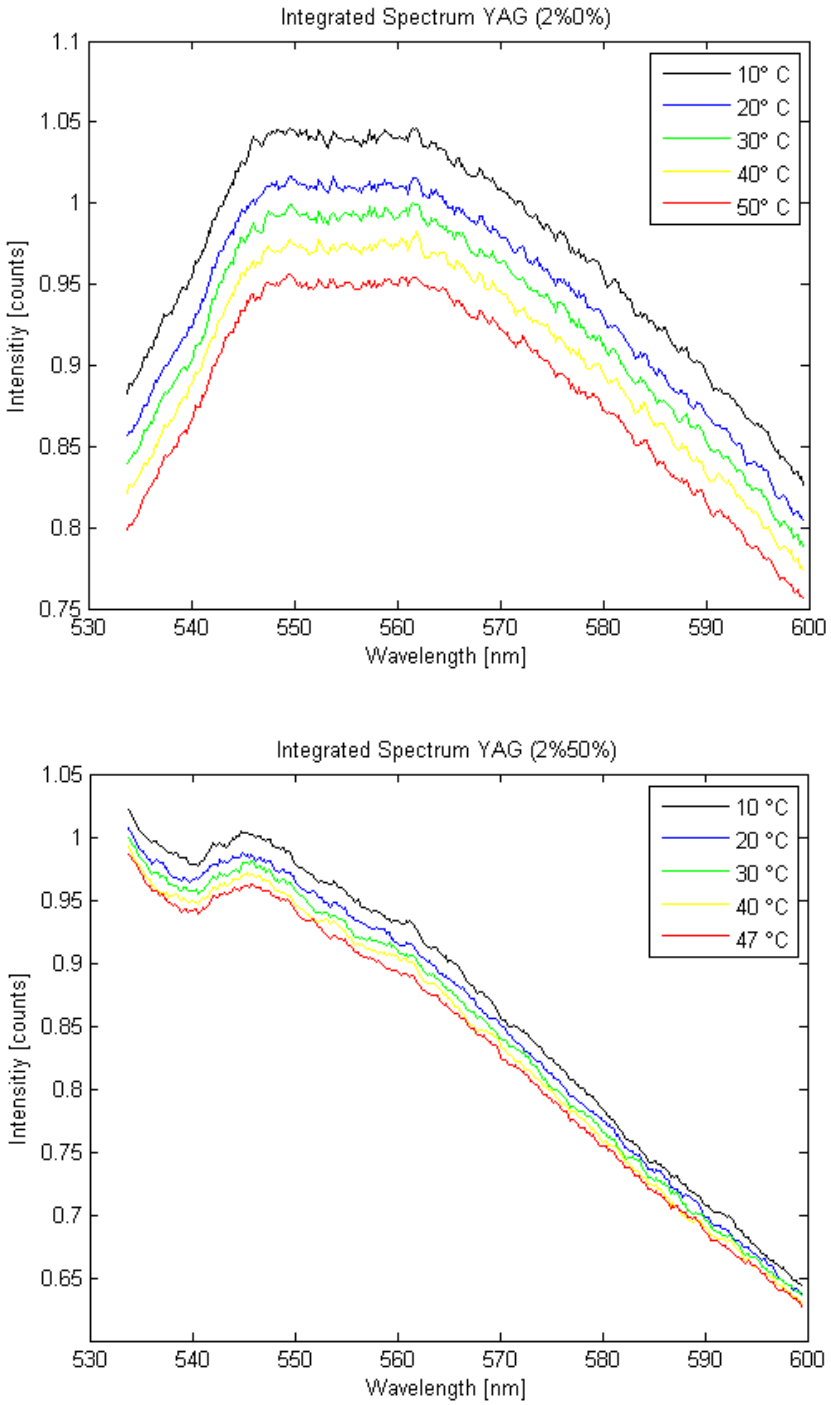

Figure 8. Phosphor Spectra

When integrating over the range of thermal sensitivity, approximately 535 nm to 600 nm, the calibration coefficients of the phosphor can be determined. This range was chosen because these are the bounds over which there will be no excitation light or

luminophore emission altering the signal. The calibration results are summarized in Table 1.

Table 1. Thermographic Phosphor Candidates $(Y_{1-x}Ce_x)_3(Al_{1-y}Ga_y)_5O_{12}$

Phosphor	Temperature Sensitivity	Ease of Application
X = 0.01 Y = 0.5	-0.028% per °C	Difficult to maintain suspension
X = 0.01 Y = 0.75	-0.851% per °C	Difficult to maintain suspension
X = 0.02 Y = 0	-0.240% per °C	Mixed the best with P/C
X = 0.02 Y = 0.5	-0.104% per °C	Difficult to maintain suspension

Other possible criteria that contribute to phosphor selection are as follows. If the thermal sensitivity of the phosphor matches that of the luminophore, the pressure signal can be normalized by the thermal signal and all temperature effects would be removed. This can only be achieved if proper concentration levels and phosphors with the proper thermal sensitivity are used. An additional consideration is the lifetime of the phosphor. In this case, the lifetime of the phosphor should be as short as or shorter than that of the luminophore. The lifetime of the paint determines the minimum exposure time in unsteady measurements and currently the lifetime of the luminophore is the limiting factor so the phosphor in an ideal paint would have a lifetime shorter than the luminophore to preserve the paints properties. The two luminophores used most with polymer-ceramic paints are Ruthenium complexes with a lifetime on the order of 10 μs and Platinum complexes on the order of 100 μs. YAG:Ce phosphors have considerably smaller lifetimes on the order of 50 ns.

The phosphor that was ultimately chosen was the one with the highest thermal sensitivity. Here it is clear that the YAG(Ce) phosphor with 1% Ce and 75% Ga content is the most thermally sensitive of the group tested.

DUAL-PAINT CALIBRATION

Experimental Setup

The OSU AARL utilizes a custom built calibration chamber to characterize all of the PSP formulations manufactured at the lab. The chamber is an aluminum enclosure that is both pressure and temperature controlled and hydraulically cooled. A 1”x1” sample coupon is placed onto a copper plate; the other side of that plate is an embedded Thermo-electric Cooler. The sample holder also has optical access and is connected to both high pressure air and a vacuum pump. Both temperature and pressure can be independently controlled by the user and paint can be completely characterized. This chamber has an operational envelope of 3-50° C and 10-200 kPa.

This calibration chamber is placed inside a dark chamber with an optical breadboard fixture installed (Figure 9). Any assortment of excitation and measurement sources can be implemented. For the presented data a single ISSI 480 nm pulsed LED array was used as an excitation source for the paint. Both an Apogee Alta U2000C color camera and an Ocean Optics USB4000 spectrometer were used. The Apogee Alta camera uses a Nikkon 35mm 1:2.8 lens with Andover 515nm long pass and 675nm short pass filters. The long pass filter’s purpose is to attenuate the excitation source. The short pass filter was used to eliminate the portion of the PtTTFP emission spectra that overlaps into the green channel absorption spectrum in the IR region. The quantum efficiency of the CCD chip was used to correlate the emission of the paint to the absorption of the camera pixels. It was necessary, because of some signal overlap, to select optical filters (Figure 11).

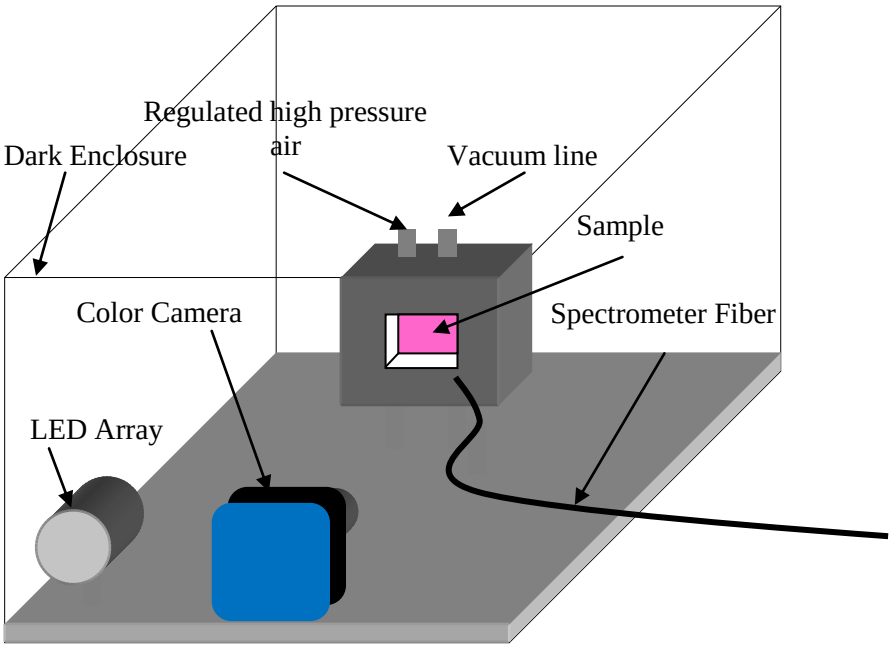

Figure 9. Calibration Setup

The sample was prepared as a fast polymer-ceramic paint with a titanium dioxide base that has been tested thoroughly and has proven to be robust. This paint has a base coat that is composed of a slurry of micro-scale titanium dioxide particles suspended in water in a 1.62:1 weight ratio. Upon application to the surface, the particles are coarsely bound together with a polymer binder in a 3% weight fraction. Once this basecoat is applied to a surface, a series of phosphor coatings were applied. These phosphor coatings were a simple suspension of 1% phosphor in methanol. This suspension was difficult to create due to rapid settling of the phosphor. First the phosphor particles were broken up and reduced in size with a mortar and pestle. Samples of the phosphor were ground until no visible clusters were present. This powder was then suspended in methanol at a 1% weight fraction and sonicated for a duration of approximately 1 hr to break up additional particles. This suspension was moderately stable and proved to be sufficient for use in an

airbrush. The phosphor was sprayed onto the basecoat until a slight yellow color appeared. The luminophore was sprayed on top of this coat to finish the paint preparation. Additional samples were created by substituting the phosphor into the ceramic base coat, unfortunately the amount of phosphor required was too high and settling issues prevented this method from producing viable samples. A smaller particle size and a more thorough study might produce a viable paint with a thermographic phosphor integrated into the ceramic substrate.

During the calibration, both the camera and spectrometer were set with an exposure time of 300 ms which produced sufficient signal strength while remaining below the saturation points of the devices. The excitation source was driven with 10 ms pulses at a duty cycle of 20%. The coupon was centered in the cameras view and an appropriate zoom was utilized where almost the entire view of the camera was filled with the sample.

Results

The spectra seen in Figure 10 were collected from the Ocean Optics USB spectrometer. Here the mechanics of the paint can be visualized.

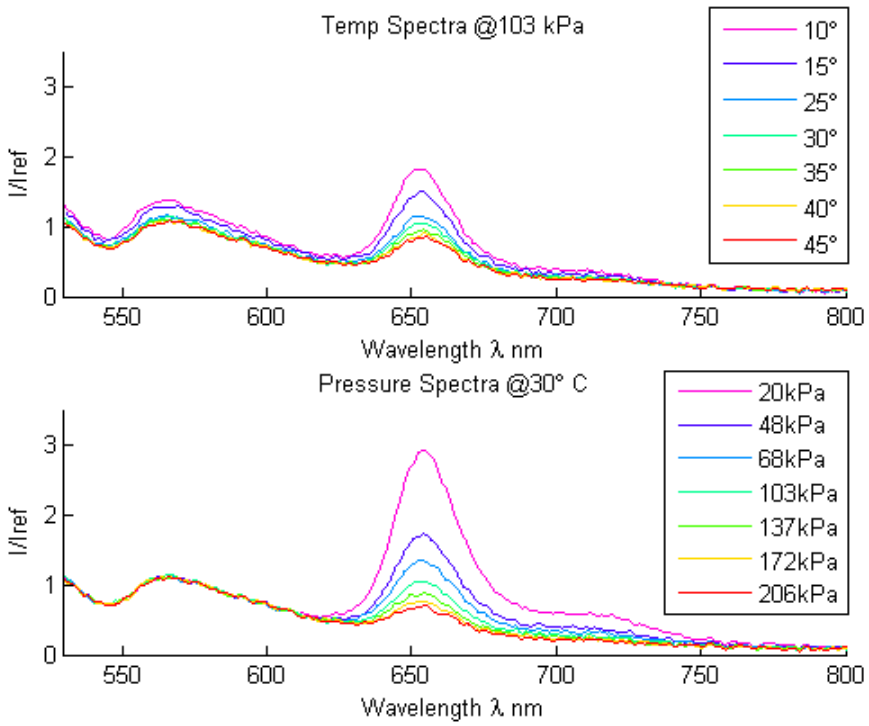

Figure 10. Emission Spectra of the YAG Phosphor and PtTFPP

The spectra are normalized to the reference condition of 103 kPa and 30°C. The magnitude of the pressure and temperature sensitivity can be easily visualized showing how the phosphor with an emission peak at 560 nm is insensitive to pressure and the pressure sensitivity of the luminophore is greater by a factor of 1.5 than its temperature sensitivity. This knowledge of the exact spectra can be used to evaluate the ability of the CCD camera to capture the thermal and pressure signals. The quantum efficiency of the CCD camera is shown in Figure 11. It is clear that the green channel only is exposed to the thermally sensitive region with a maximum wavelength detected of 610 nm where the pressure sensitive region begins to emit at 625 nm. A 675 nm short pass filter is added because the green channel absorption steadily increases starting at 675 nm into the infrared which would detect the pressure sensitive region of the paint from 675 nm to 750

nm seen in Figure 10. However, the phosphor emission spectrum overlaps into the red channel which reduces the pressure sensitivity by adding non pressure sensitive signal.

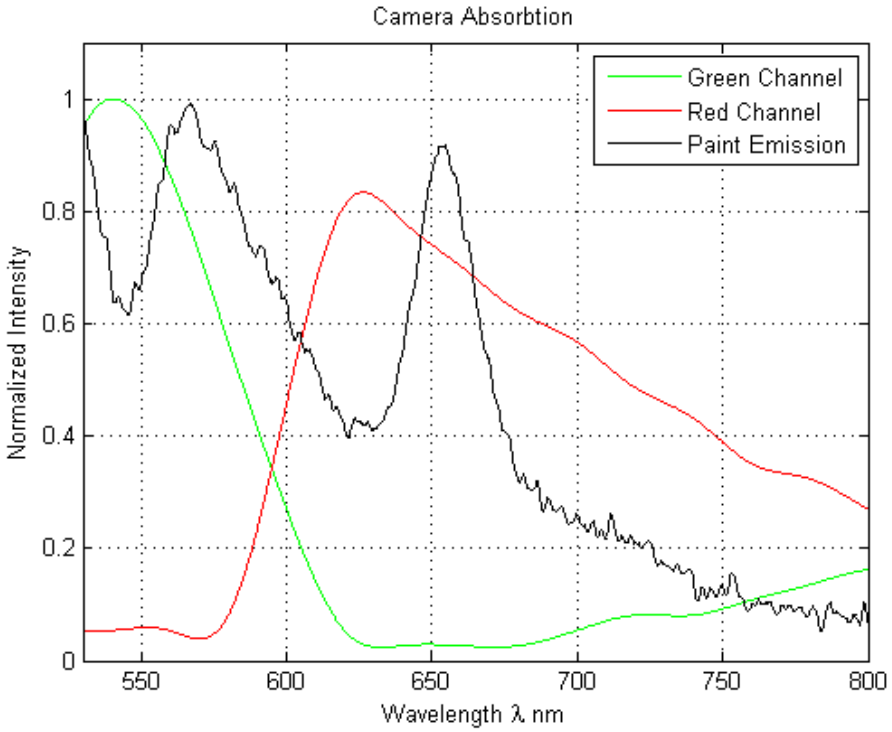

Figure 11. Quantum Efficiency of the CCD color camera used [10]

When the camera images are integrated and only the green channel used, the temperature sensitivity of the phosphor itself can be determined. Figure 12 shows the thermal sensitivity of the phosphor. The reference condition here is at 103 kPa and 30°C.

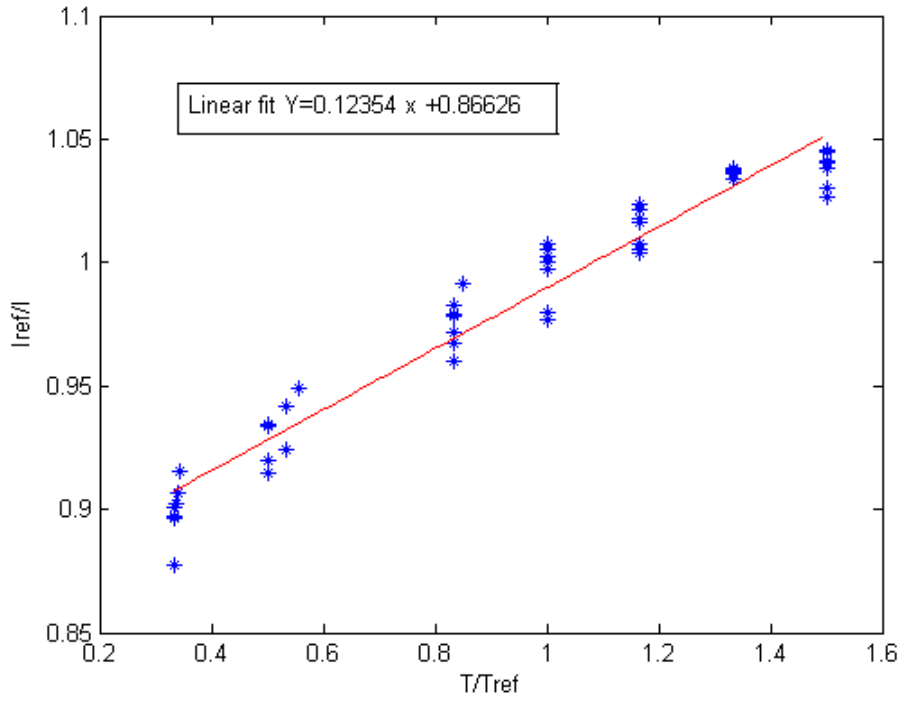

Figure 12. Calibration Curve from the Green Signal

The paint sample calibrated in the chamber quantified the significant temperature sensitivity of the luminophore in a polymer ceramic PSP setup. The error in indicated pressure was created by a thermal difference was characterized by determining the change in indicated pressure with a discrete change in temperature. I_{ref}/I represents the intensity ratio of either a pressure or temperature effect on the PSP. ΔP is the change in indicated pressure as a result of temperature change in the paint. ΔT is the change in temperature from the reference condition that influences the paint emission.

$$\frac{\left(I_{ref}/I\right)_{pressure}}{\left(I_{ref}/I\right)_{temp}} \approx \frac{\Delta P}{\Delta T} = E_{pressure} \qquad \textbf{Equation 4}$$

The error introduced in the pressure value indicated by the paint was 3 kPa/°C. This characterizes the uncompensated thermal sensitivity of the luminophore and the source of

significant error in the indicated pressure present with thermal effects. Because the emission intensity of both the phosphor and luminophore are inversely proportional to the temperature, normalizing the luminophore emission intensity by the phosphor emission intensity reduces the overall thermal sensitivity. In a paint where the thermal sensitivity of the luminophore and phosphor are matched, this temperature error would disappear completely. The thermal sensitivity of the phosphor can also be used to determine the exact temperature of the paint at any given point in time.

This temperature error can be visualized when looking at constant intensity lines for a two-dimensional calibration presented in Figure 13. In an experiment, the raw data obtained from a painted surface is the intensity ratio at a point. The data point that is extracted from a typical PSP test can be represented as a single iso-intensity line in Figure 13. In this particular case the reference condition is at 30°C and 103kPa. If the data point yields an intensity ratio of 1.05 and there is no temperature shift from the reference condition, solving for the pressure is a simple 1-d problem. However if there are any unknown temperature effects the actual data point could lie anywhere on the 1.05 line. If this is not accounted for the indicated pressure would be dramatically different from the actual experimental value.

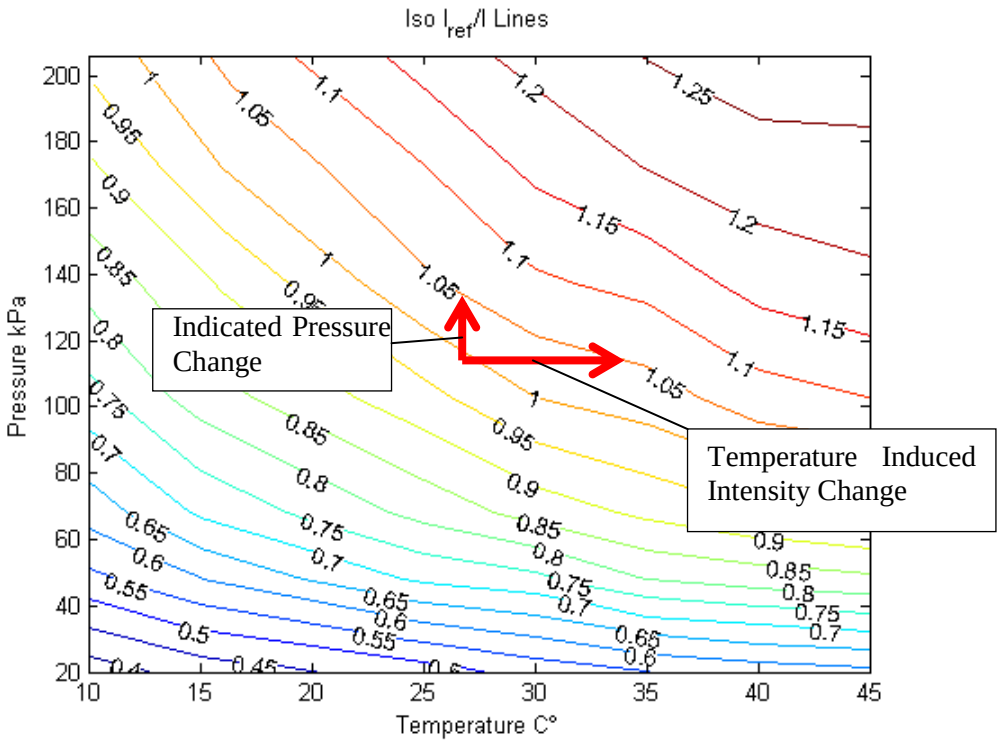

Figure 13. Temperature Error Determination

Looking at Figure 13 it is visible that PtTFFP in a polymer-ceramic paint has a nonlinear response to both temperature and pressure. This means that simply using a pressure tap to correct for an intensity shift is not enough to completely remove the sensitivity as the pressure sensitivity changes as a function of temperature, becoming more sensitive as the temperature decreases. Using this and an in depth 2-dimensional calibration of the luminophore, the temperature error can be removed completely. This technique requires the complete calibration of both the phosphor and luminophore over the range of testing pressures and temperatures which may not be possible in all situations. This method also requires more thorough data processing which might perpetuate the growth errors in data acquisition.

There is an alternative method in which a local region over which the thermal sensitivity is mitigated is created. As mentioned earlier, normalizing the pressure signal

by the phosphor signal will reduce the thermal sensitivity of the pressure signal because both signals are thermally sensitive. However this can be taken a step further if the properties of the luminophore and phosphor are known, particularity the explicit thermal sensitivity of both molecules. Knowing both of these sensitivity factors the phosphor signal can be artificially sensitized by increasing the magnitude of the intensity ratio. This method assumes that both the sensitivity of the phosphor and luminophore is linear, but this is not the case so the result only works for a region where the linear assumption holds true. This sensitivity factor is the linear change in intensity ratio versus the temperature ratio as seen in equation 5.

$$\overline{K} = \frac{\Delta {I_{ref}}/{I}}{\Delta {T}/{T_{ref}}} \qquad \textbf{Equation 5}$$

Here an arbitrary change in intensity ratio is normalized by the corresponding temperature ratio. A series of these points are taken throughout the 2-d calibration of the paint. These values are then averaged to yield as single sensitivity factor. It was mentioned that the luminophore has a nonlinear reaction to thermal changes, this is ignored in this case. Once the sensitivity for both the phosphor and luminophore are known, a simple conversion is used to alter the phosphor signal such that its sensitivity is the same as the luminophore's.

$$\left({I_{refP}}/{I}\right)_{Corr} = 1 - \left(1 - {I_{refP}}/{I}\right) \times \frac{\overline{K}_{\text{Luminophore}}}{\overline{K}_{\text{Phosphor}}} \qquad \textbf{Equation 6}$$

The corrected pressure signal is achieved by normalizing the raw pressure intensity ratio by the corrected phosphor signal.

$$\left(I_{refL}/I\right)_{Corr} = \frac{\left(I_{refL}/I\right)}{\left(I_{refP}/I\right)_{Corr}}$$

Equation 7

While using this correcting scheme a similar plot of constant intensity ratio lines is shown in Figure 14 and was from the same calibration data seen in Figure 13 but normalized by the scaled phosphor signal.

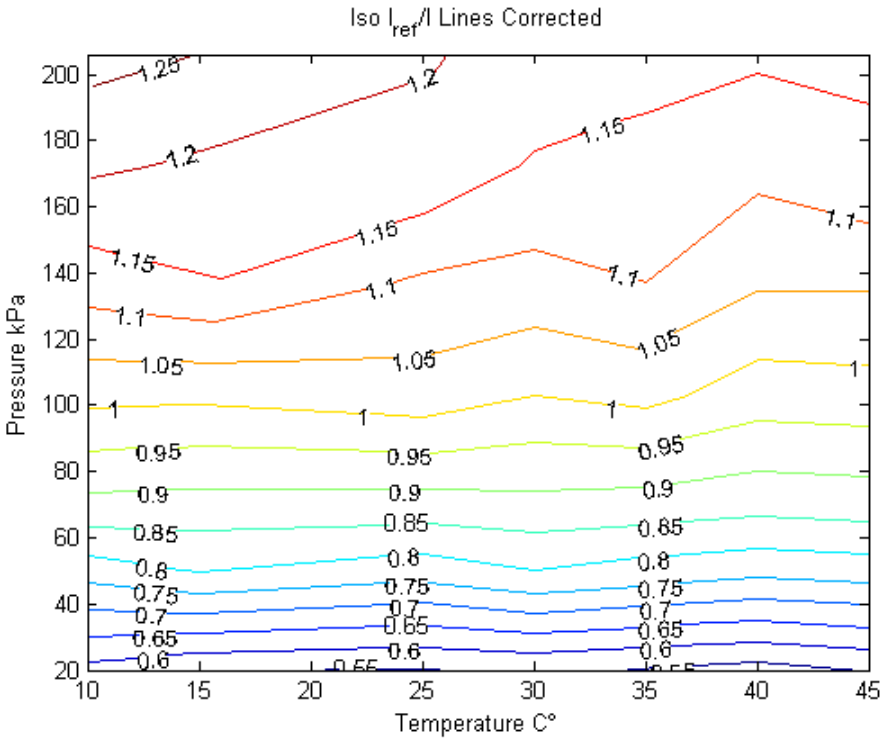

Figure 14. Temperature Error Corrected

Here it can be seen that the thermal sensitivity of the combined paint has been dramatically reduced. At pressures lower than ambient the thermal sensitivity is almost completely removed. At higher pressures the nonlinearity of the pressure sensitivity shows up. This region also is plagued by low signal levels and perhaps the non-ideal shape is due to the low signal to noise ratio in both the phosphor and luminophore signal.

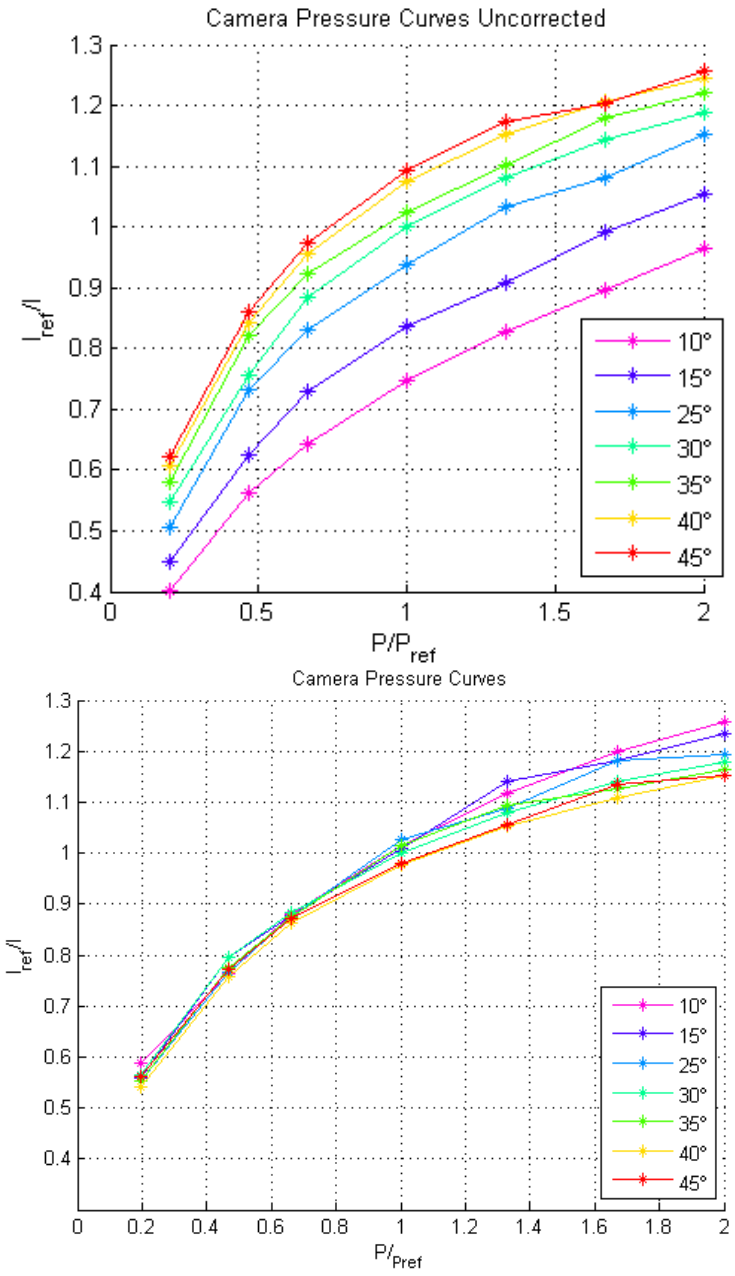

Figure 15. Isothermal Pressure Curves

Figure 15 shows the reduction of temperature sensitivity in the form of collapsing isothermal pressure curves. This can be examined further in Figure 17 where qualitatively the change in temperature sensitivity is visible whereas the change in pressure sensitivity is negligible. This temperature error can be removed more effectively

after calibrating the reference to calculate an exact temperature and then calibrating the pressure signal for multiple temperatures. However, this method cannot be evaluated solely with a calibration chamber as both pressure and temperature are known at every point and these points themselves are responsible for the calibration.

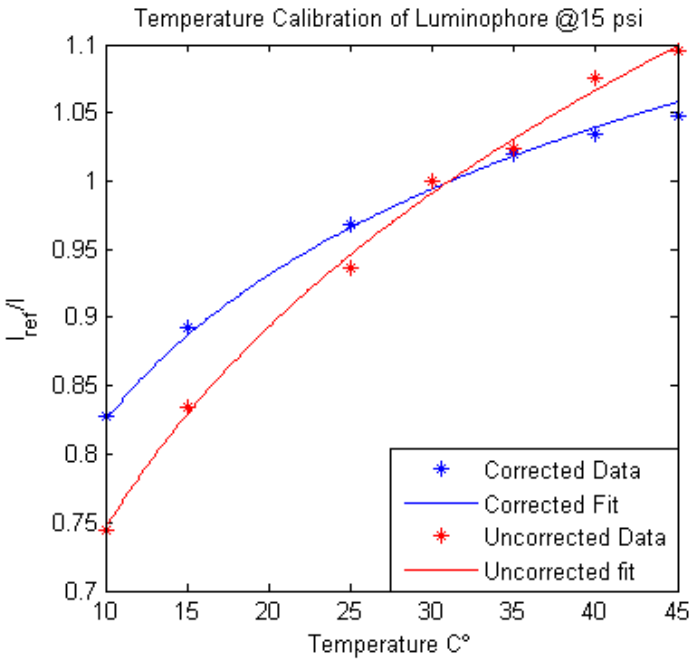

Figure 16. Temperature Calibration

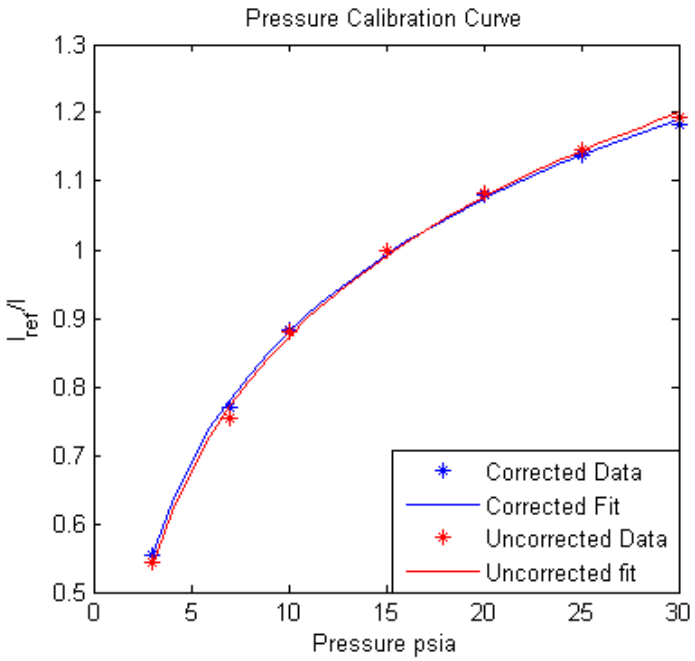

Figure 17. Pressure Calibration

These results from the calibration chamber were used to correct the wind tunnel data and produce surface plots during the run. The temperature profile was first determined using the ratio of the wind off reference image and the wind on image.

WIND TUNNEL TEST

Experimental Setup

A proof of concept test was set up at the OSU AARL 6”x22” transonic wind tunnel. This facility is capable of Mach numbers ranging from 0.2 to 1 and Reynolds numbers of 2-16 million/foot. It is a blow down facility utilizing high pressure air from tanks located at the facility. This tunnel was used because the test section experiences significant temperature changes from ambient conditions due to a falling total temperature and high speed flows. The test section is two-dimensional and designed to evaluate airfoil cross-sections. Optical access is granted through two acrylic windows on both lateral sides of the airfoil test section and a small window directly above the mounted airfoil. A NACA 0021 airfoil was chosen for its significant thickness and previous use in the wind tunnel with PSP.[3]

The airfoil was coated with a polymer ceramic base coat with luminophore and phosphor coatings on the surface. Additionally, six pressure taps were located along the chord to provide a reference for the pressure signal. These taps were located at x/c values of 0.05, 0.20, 0.35, 0.55, 0.75, and 0.90. Two thermistors were surface mounted to the airfoil along the near side of the test section to provide a calibration source for the paint. These were located at x/c values of 0.25 and 0.75.

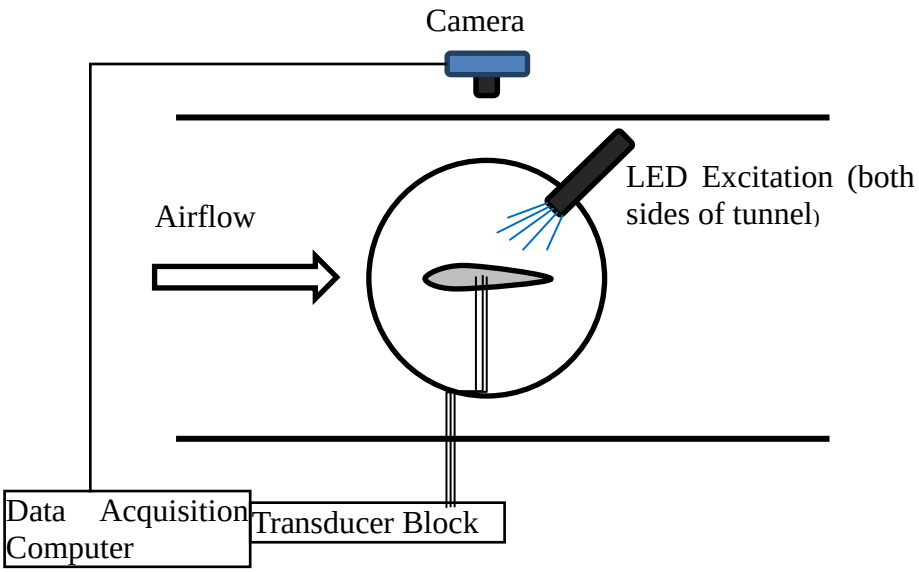

Figure 18. Wind Tunnel Setup

The painted airfoil was tested at 10º angle of attack at a Mach number of 0.6 and at a Reynolds number of 3.8 million. Pressure data was recorded using a 20 tap transducer block with a ± 45 psi rating. The same Apogee color camera with 500 nm long pass and 675 nm short pass filters attached. The excitation sources were two identical 480 nm 2-inch diameter ISSI LED arrays. The LED's were operated in a constant excitation mode. When preparing the airfoil, there was difficulty encountered applying the phosphor coating to the paint. This is most likely a result of the particle size of the phosphor in suspension. The solution was very dilute and consistently agitated to prevent phosphor sediment from building up when sprayed. This led to a very clear solution not visible on the surface of the basecoat. When too much solution was applied too quickly, the surface tension of the methanol would cause the solution to bead up on the surface leading to a higher concentration of phosphors at the edge of the bead. This was difficult to avoid even when aware of this complication. The airfoil was repainted to produce a more even distribution.

Each wind tunnel run consisted of a series of dark and reference images prior to the blow-down valve opening. Once the valve opens, the airflow accelerates until the choke vanes downstream choke the flow. Once this condition is reached a series of wind on images were taken while the Mach number remained fixed at 0.6. In addition to images, the pressures on the airfoil and total and static pressure of the test section were measured from the pressure transducer block. The valve is closed and the flow stopped. Following this a second set of wind off images were taken. For every image acquisition, a set of pressure and thermistor data was acquired.

Results

Figure 19 shows the temperature distribution for the NACA 0021 airfoil in Mach 0.6 flow at an angle of attack of 10º. The data was filtered with a moving disk filter with a 5 pixel radius. A 2-point linear calibration was used to calibrate both temperature and pressure. The 2-point thermal calibration was created using the 2 embedded thermistors as thermal point sources. Once the pressure signal had been normalized, 2 pressure taps were used to calibrate for pressure.

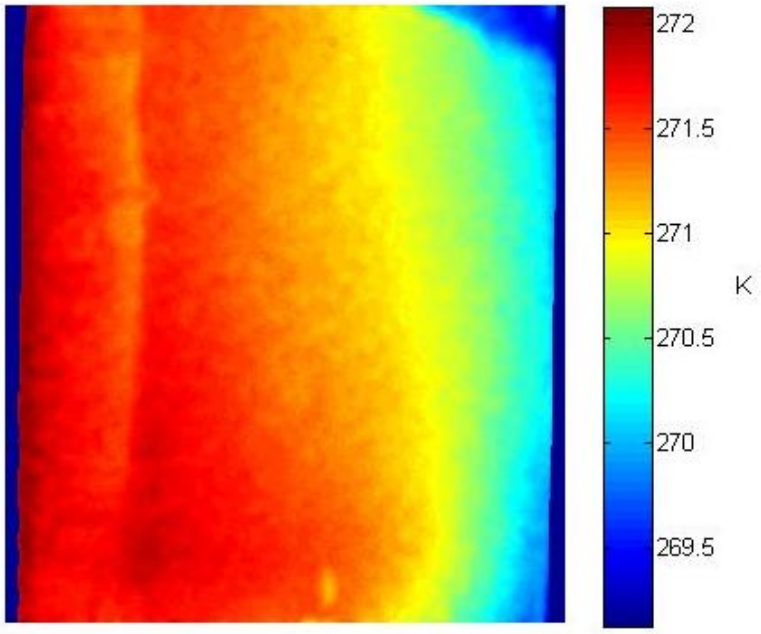

Figure 19. Temperature (K) at M=0.6 α= 10º (flow from left to right)

It is clearly visible that at the stagnation point and the near leading edge, there is a slight temperature increase from the total temperature of the run, 293 K, being higher than ambient conditions, 280 K. Spanwise, there is little deviation because of the high thermal conductivity of the aluminum airfoil. However, the end plates on the airfoil are different; the top side is a solid aluminum block and the bottom side has an inch diameter cylinder mounting the airfoil against the wall. The thermal capacity is different leading to about a 0.5 degree difference. The pressure signal can be partially corrected for thermal effects by simply dividing out the corrected thermal intensity ratio.

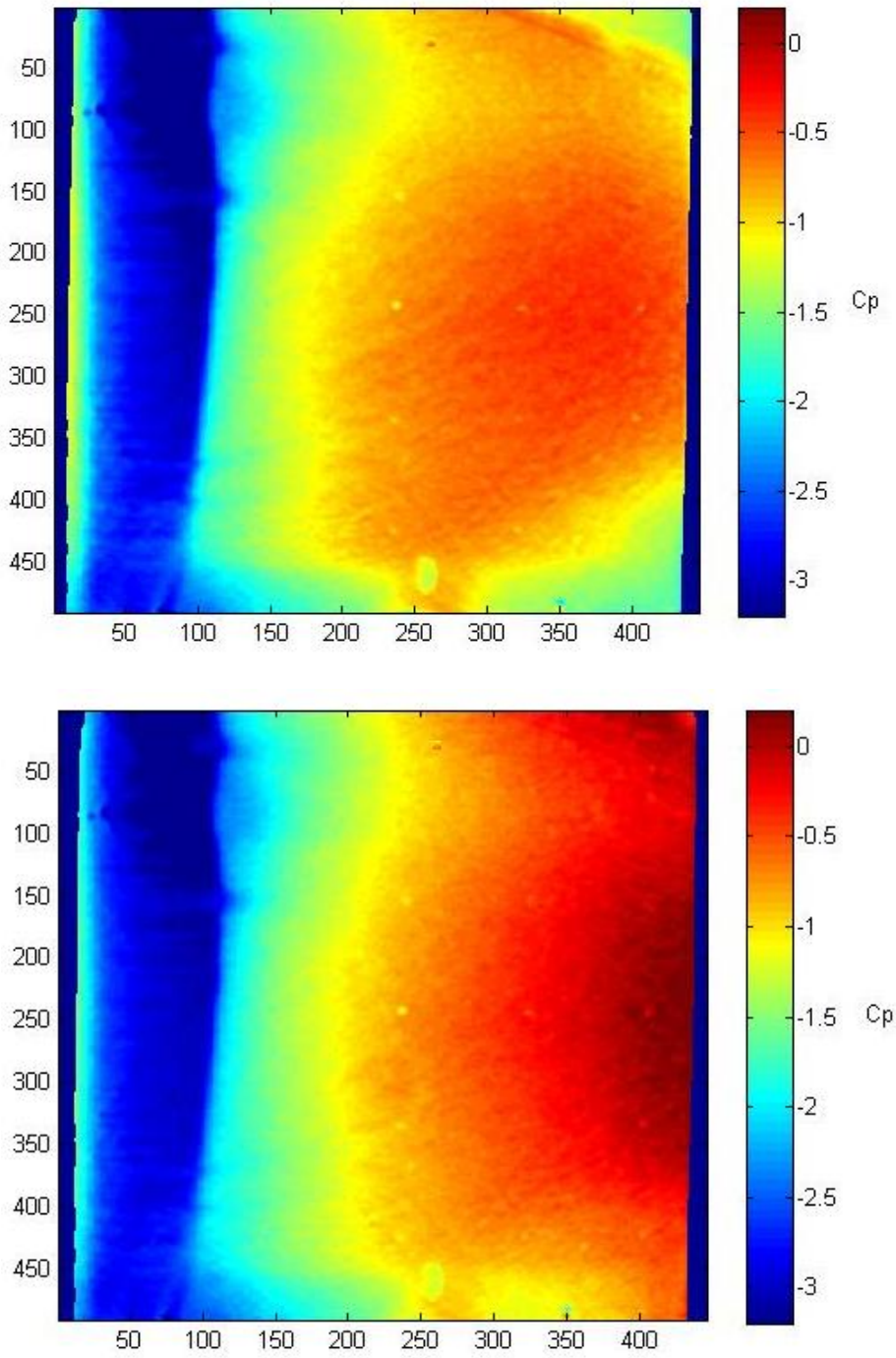

Figure 20. I_{ref}/I of the Pressure Signal, Unreferenced (Top) Referenced (Bottom)

Figure 20 shows how the pressure does not fully recover at the trailing edge of the airfoil and yet once the image is referenced by the temperature information, the pressure

recovers in the correct direction. Additionally there are some spanwise temperature induced errors. These can be seen in the upper right and lower right corners and they too are removed once the image is referenced. Some features of the flow over an airfoil can be seen such as the strong shock at quarter chord and the resulting pressure spike. This shock is also visible in the thermal distribution, demonstrating the thermal increase in the wake of a shock. The intensity ratio can be converted to a pressure ratio using the Stern-Volmer relation, Equation 2, except the temperature ratio is replaced with a pressure ratio. The pressure ratio is converted into the coefficient of pressure, *Cp*, by the following relation.

$$C_p = \frac{P/P_{ref} - 1}{1/2 M^2} \qquad \textbf{Equation 8}$$

M represents the free stream Mach number and *P* is the local static pressure and P_{ref} is the free stream static pressure. The 15 pixel spanwise average of the center chord line pressure coefficient is presented Figure 21 along with the data from the pressure taps along the chord.

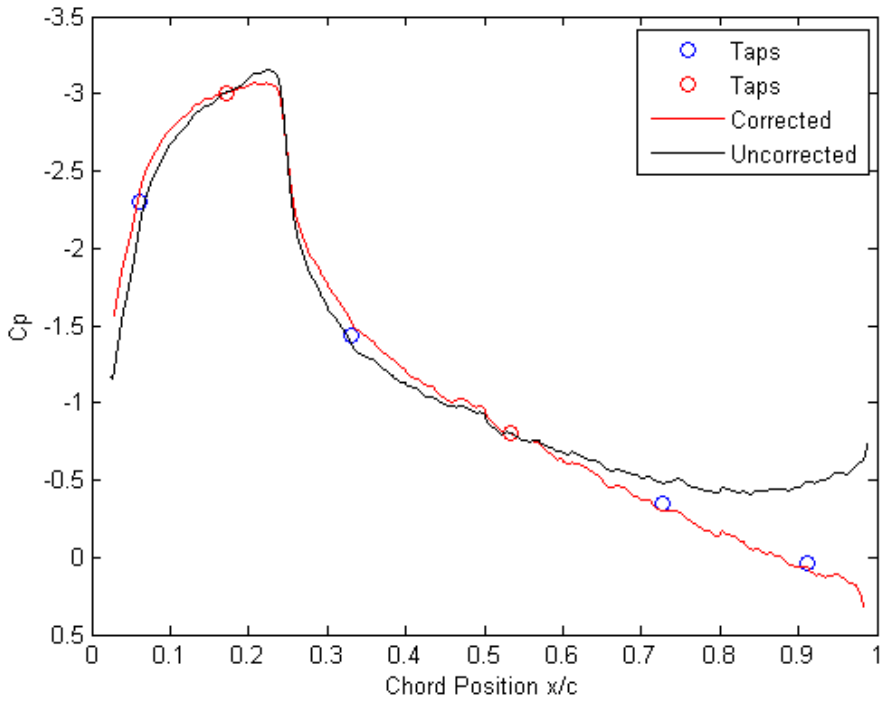

Figure 21. Coefficient of Pressure Comparison

Taps 2 and 4 (colored red in Figure 21) were used as the 2 point pressure calibration sources. The tap locations were determined by visually locating the pixel location of the pressure taps and correlating them to the measured location as a percentage of distance along the chord. This calibration technique removes any bias error cause from a thermal shift between the wind on and wind off images and calibrates the data for the temperature present at the two taps. The quality of the data processing technique can then be visualized when comparing the unused pressure taps with the indicated PSP data. This is why the uncorrected pressures data corresponds closely with the pressure taps over most of the span, but diverges at the trailing edge of the airfoil. The trailing edge of the airfoil has a dramatic temperature gradient seen in Figure 19. The strong normal shock present at quarter chord is easily visible in the *Cp* plot as well showing a sharp increase in pressure.

CONCLUSION

These experiments demonstrate an alternate method for temperature correction in pressure-sensitive paint systems. The thermographic phosphor $(Y_{0.99}Ce_{0.01})_2(Ga_{0.75}Al_{0.25})_5O_{12}$ proved to be a feasible reference source that successfully alleviated excessive temperature errors in a PSP measurements. These errors were demonstrated in a calibration setup along with a wind tunnel test. In both cases the reference signal was sufficient to dramatically reduce the thermally based errors in pressure measurements. These tests also proved that this new paint formulation is a sufficient substitute for platinum based polymer-ceramic PSP's over a pressure range of about 150 kPa – 5 kPa and a temperature range of -10 – 50 C. This range is very expansive for a single PSP system.

Without using any *a priori* calibrations and two points of known pressure and known temperature, the pressure map was completely recovered in the wind tunnel test. This is significant because *a priori* calibrations are often very specific to the paint used and the testing environment. Having a system that only requires two pressure taps and two thermal taps is extremely versatile in the experimental fluid dynamics world.

This new paint system requires very little change to be made to the current PSP testing structure. The paint utilizes the same excitation source of 480 nm blue LED's. The paint application is only slightly altered; it maintains the same basecoat and luminophore coat procedures with the addition of a phosphor coat. The camera procedure was only slightly altered. A new set of optical filters were used in comparison to the traditional PSP method in addition to swapping the gray scale camera with a color camera.

Further work includes incorporating the phosphor directly into the ceramic structure of the base coat which was never successfully achieved in the testing presented here. If this is feasible, the paint preparation process would be dramatically simplified while increasing the control of the phosphor concentration. This could be achieved with experimentation of phosphor particle size and chemical dispersants. The paint also needs to be evaluated over a larger range of pressures and temperatures to evaluate the range of testing that it can cover. Other work includes applying the paint to a more controlled and static test where the true sensitivity of the paint can be evaluated and compared directly to theory and historical evidence. Alternative methods of data post processing could be utilized with the current paint system. These methods were outlined in the background section of this report and would involve using a full *a priori* calibration instead of local reference points on the model to extract the data. A second method that was discussed was using this paint in a lifetime method, where the luminescent decay of the phosphor would be evaluated as a thermal reference signal.

REFERENCES

[1] Bell, J.H., Schairer, E.T., Hand, L.A., and Mehta, R.D., "Surface Pressure Measurements Using Luminescent Coatings," *Annual Review of Fluid Mechanics,* Vol. 33, 2001, pp. 155-206.

[2] Fang, S., Disotell, K.J., Gregory, J.W., Semmelmayer, F.C., and Guyton, R.W., "Unsteady Surface Pressure Measurements on a Hemispherical Dome with Pressure-Sensitive Paint," *10th International Conference on Fluid Control, Measurements, and Visualization,* 2009.

[3] Gompertz, K., Kumar, P., Jensen, C.D., Peng, D., Gregory, J.W., and Bons, J.P., "Modification of a Transonic Blowdown Wind Tunnel to Produce Oscillating Freestream Mach Number," *48th AIAA Aerospace Sciences Meeting Including the New Horizons Forum and Aerospace Exposition,* AIAA-2010-1484, Vol. 48th AIAA Aerospace Sciences Meeting Including the New Horizons Forum and Aerospace Exposition, AIAA, 2010.

[4] Gregory, J.W., Asai, K., Kameda, M., Liu, T., and Sullivan, J.P., "A Review of Pressure-Sensitive Paint for High-Speed and Unsteady Aerodynamics," *Proceedings of the Institution of Mechanical Engineers, Part G: Journal of Aerospace Engineering,* Vol. 222, No. 2, 2008, pp. 249-290.

[5] Crafton, J., Fonov, S., Jones, E., Goss, L., and Carter, C., "Bi-Luminophore Pressure-Sensitive Paint Development," *8th Annual Pressure Sensitive Paint Workshop,* NASA Langley Research Center, Langley, VA, 2000.

[6] Allison, S.W., "Nanoscale Thermometry via the Fluorescence of YAG:Ce Phosphor Particles: Measurements from 7 to 77 ◦C," *Nanotechnology,* Vol. 14, No. 8, 2003, pp. 859.

[7] Allison, S.W., "A Survey of Thermally Sensitive Phosphors for Pressure Sensitive Paint Applications." *Proceedings of the International Instrumentation Symposium,* Vol. 46, 2000, pp. 29.

[8] Hansel, R.A., Allison, S.W., and Walker, D.G., "Temperature-Dependent Luminescence of Gallium-Substituted YAG:Ce," *Journal of Materials Science,* Vol. 45, No. 1, 2010, pp. 146.

[9] Goss, L., Jones, G., Crafton, J., and Fonov, S., "Temperature Compensation in Time-Resolved Pressure Measurments," *International Symposium of Flow Visualization,* 2004.

[10] Anonymous "Kodak KAI-2020 Image Sensor: 1600[H] x 1200[V] Interline CCD Image Sensor," Eastman Kodak Comapny, 3.0 MTD/PS-0692, 2007.